

Dark Matter prospects with COSI: ALPs, PBHs and sub-GeV Dark Matter

Andrea Caputo,^{a,b} Michela Negro,^{b,c,d} Marco Regis,^{f,g} Marco Taoso^g

^aSchool of Physics and Astronomy, Tel-Aviv University,
Tel-Aviv 69978, Israel

^bUniversity of Maryland, Baltimore County, Baltimore, MD 21250, USA

^cNASA Goddard Space Flight Center, Greenbelt, MD 20771, USA

^dCenter for Research and Exploration in Space Science and Technology, NASA/GSFC,
Greenbelt, MD 20771, USA

^fDipartimento di Fisica, Università di Torino, via P. Giuria 1, I-10125 Torino, Italy

^gIstituto Nazionale di Fisica Nucleare, Sezione di Torino, via P. Giuria 1, I-10125 Torino,
Italy

E-mail: andreacaputo@mail.tau.ac.il, mnegro1@umbc.edu, marco.regis@unito.it,
marco.taoso@to.infn.it

Abstract. We study the prospects in the search of dark matter offered by the newly selected NASA MeV mission COSI (Compton Spectrometer and Imager). This instrument is designed and optimized to detect spectral lines, and we show it offers an exquisite possibility to detect dark matter directly decaying or annihilating into monochromatic gamma-rays. This is the case, for example, for axion-like particles (ALPs) which undergo decay into two photons. Furthermore, we show that COSI can lead to important progress in the quest for primordial black holes (PBHs) dark matter, through measurements of the 511 keV line from the positrons produced via Hawking evaporation. We also outline opportunities for the search of continuum signals, such as those expected from sub-GeV dark matter annihilation/decay into leptons and PBH evaporation into photons. We find that also in this case COSI can lead to improvements of current bounds.

Contents

1	Introduction	1
2	Spectral line signatures	2
2.1	Decay	2
2.2	Annihilation	6
3	Continuum signals	6
3.1	Primordial black holes evaporation	7
3.2	Annihilation and decay of sub-GeV DM into leptons	9
4	COSI, dark matter and the Galactic Center 511 keV gamma-ray line	10
5	Conclusions	13

1 Introduction

The MeV gamma-ray energy range is one of the frontiers in observational astronomy, with huge implications for the understanding of high-energy astrophysical phenomena and involving significant activity for the next-generation of instruments. Indeed, several mission concepts have been developed in the past decades with main focus to observe the so-called *MeV gap*, a ‘gap’ in sensitivity between ~ 100 keV and ~ 100 MeV. Some examples that appeared in literature are AMEGO [1], (e-)ASTROGAM [2, 3], COSI [4], AMEGO-X [5], ETCC [6]. These mission concepts aim to improve the sensitivity in the MeV band which is currently covered only by the observations of the COMPTEL [7] on board of the NASA’s Compton Gamma-ray Observatory (CGRO, [8], decommissioned after 9 years of operation in 2000) and INTEGRAL/SPI ([9], which out-perform COMPTEL sensitivities below 2 MeV).

In this work we focus our attention on the mission concept that have been recently selected by NASA as the next SMEX: the Compton Spectrometer and Imager, COSI [4, 10]. This mission, currently in Phase B of the NASA’s Project Life Cycle, will have important implications for physics and astrophysics, from stellar nucleosynthesis to the production of antimatter (positrons) in our Galaxy, to jets formation and mechanisms in gamma-ray bursts, blazars and compact objects, and – as we prove in this work – it can also lead to dark matter (DM) discovery.

COSI is a wide field of view gamma-ray telescope that allows unprecedented high-resolution spectrometry in the 0.2–5 MeV energy range thanks to cryogenic germanium detectors. COSI detects high-energy photons that Compton scatter in the detectors and, hence, it has inherited imaging capabilities with angular resolution that well meet the requirements of 3.8° full width at half maximum (FWHM) at 0.511 MeV and 2° FWHM at 1.809 MeV. Scheduled to be launched in 2027, COSI will survey the sky orbiting Earth at 550 km altitude along an almost equatorial orbit, with a North-South rocking, which will assure a daily full-sky coverage.

The design of the instrument is optimized to resolve the antimatter distribution in the center of our galaxy through the 511 keV e^+e^- annihilation emission line; to provide major advances in nuclear line studies, in particular from ^{26}Al , ^{60}Fe and ^{44}Ti radionuclides, tracing

element formation, past core-collapse supernovae activity, and new supernovae explosions, respectively; to measure polarization of photons emitted in extreme environments which will provide insights on the gamma-ray production mechanisms and the emission regions geometry; to probe gravitational-waves counterparts. Obviously, COSI’s potential is not limited to these main objectives, and in this paper we investigate COSI’s capabilities in the search for DM.

In fact, various DM models predict the production of gamma-ray photons in the MeV range, see e.g. [11–16]. This is the case of direct DM decay or annihilation into pairs of photons, which produces narrow lines for which COSI will have an exquisite sensitivity. Other models, such as primordial black holes (PBHs) [17–21] or DM decay/annihilation into leptons, will instead produce a continuum photon signal, which can be investigated as well by COSI, even though with a somewhat weaker constraining power. All these scenarios can inject positrons that, after cooling, can annihilate with thermal electrons to produce a 511 keV line in the Galaxy [22], and this possibility can be tightly constrained by COSI.

In this study we derive the prospects for DM searches with COSI for all the DM candidates and signatures mentioned above.

The paper is organized as follows. In Sec. 2 we explore COSI sensitivity for line signals coming from DM decay and annihilation. We consider various targets such as the Galactic Center (GC), the Large Magellanic Cloud (LMC) and the dwarf spheroidal galaxy Draco. Then we move to the continuum sensitivity in Sec. 3; we consider, in particular, signals from PBH Hawking radiation and final state radiation from electrons/positrons originating from DM decay and annihilation. The case of the 511 keV line is analysed in Sec. 4. We finally conclude and outline future directions in Sec. 5.

2 Spectral line signatures

We first study spectral line signals, for which COSI is optimized. In all such targets, the DM has a velocity dispersion $\sigma/c < 10^{-3}$, which sets the intrinsic width of the spectral line, while the COSI spectral resolution is $\Delta E_\gamma/E_\gamma > 10^{-3}$ in the whole energy range of operation. Therefore, we can assume the DM signal to be contained in a single COSI energy bin.

2.1 Decay

Let us consider a particle DM with mass m_χ decaying directly into two photons with a rate Γ_d (this may be the case of axion-like particles, ALPs). We shall focus on the signal produced by the DM halo of a certain astrophysical object in the the field of view of the telescope. As already anticipated, the energy resolution of the instrument is much larger than the velocity dispersion of the DM in the targets that we are going to consider. Therefore, the flux of photons received by the telescope is entirely contained in the bin at energy $E_\gamma = m_\chi/2$ and reads:

$$\Phi(E_\gamma) = \frac{\Gamma_d}{4\pi m_\chi} D(\theta) \times 2, \quad (2.1)$$

where $D(\theta)$ is the so-called D-factor, which measures the amount of DM along the line of sight in the targeted object:

$$D(\theta) = 2\pi \int_0^\theta d\theta' \sin(\theta') \int_{\text{l.o.s.}} dl \rho(l, \theta), \quad (2.2)$$

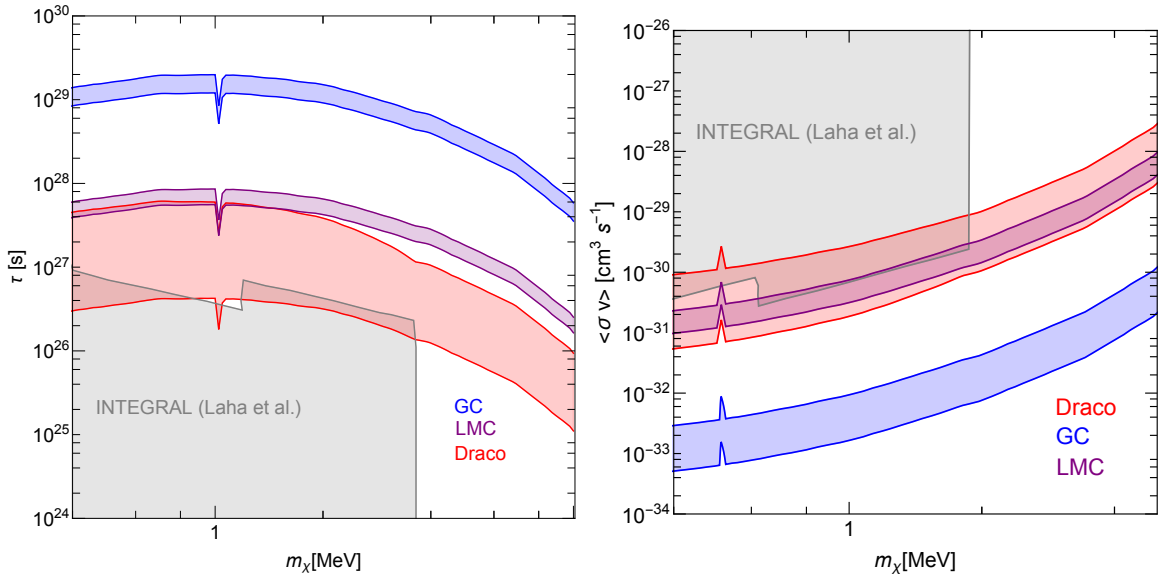


Figure 1. 3σ projected sensitivities (for 2 years of observation) for spectral line signatures in the three targets under consideration (GC, LMC and Draco), for decaying DM on the left and annihilating DM on the right. The shaded regions span the two DM density profiles considered in our analysis, see text for more details. The gray shaded region shows existing limits from [23]. COSI will therefore improve over existing bounds in both cases, probing *larger* lifetimes for decaying DM and *smaller* cross-sections for annihilating DM. Even more stringent bounds are expected when considering a larger portion of the sky analyzed with a full template analysis similarly to what done recently in [24] with INTEGRAL data.

with ρ the DM density distribution and θ the angular distance from the center of the target. For the moment, we consider the integral over a single observational angular beam, i.e. we take θ to be the half width at half maximum (HWHM) of the angular resolution measure (ARM) of the Compton telescope. Notice that here we assume $\chi \rightarrow \gamma\gamma$, however in some models the decay can actually produce only one detectable photon, $\chi \rightarrow X\gamma$. Assuming $m_X \ll m_\chi$, the latter case can be described by the same Eq. (2.2) without the factor of 2. This is actually the case for a few motivated examples [15], such as dipole DM, where the dipole operator $\frac{\lambda}{\Lambda} \bar{\chi}_2 \sigma^{\mu\nu} \chi_1 F_{\mu\nu}$ mediates the decay $\chi_2 \rightarrow \chi_1 \gamma$, hidden photino DM which decays to a photon and a gravitino, gravitino DM decaying into a neutrino and a photon, sterile neutrinos DM decaying into a photon and a light active neutrino.

To derive the projected sensitivity on the DM lifetime $\tau = 1/\Gamma_d$ as a function of the DM mass m_χ , we consider the 3σ line sensitivity for point sources $\Phi_{\text{exp}}(E_\gamma)$ reported in Figure 2 of [25], and corresponding to 24 months of COSI survey. For point-like sources we can thus directly compare the outcome of Eq. (2.2) with $\Phi_{\text{exp}}(E_\gamma)$ to obtain the sensitivity on τ :

$$\tau = 1.6 \times 10^{28} \text{ s} \frac{D}{10^{23} \text{ MeV cm}^{-2}} \frac{10^{-6} \text{ cm}^2 \text{ s} \text{ 1 MeV}}{\Phi_{\text{exp}} m_\chi}, \quad (2.3)$$

where Φ_{exp} is evaluated at $E_\gamma = m_\chi/2$ and the angular integration for D is given by the COSI angular resolution at E_γ as specified before. For reference, we provide the values of D at 1° for the targets under investigation in Table 1. To bracket the uncertainty in its determination we consider two cases, one more promising and one less promising, for each

target: NFW and Isothermal profiles for LMC (with parameters from [26]) and GC (taking $\rho_{\odot} = 0.4 \text{ GeV/cm}^3$ [27] and $r_s = 4.38 \text{ kpc}$ (Isothermal) and $r_s = 24.42 \text{ kpc}$ (NFW) [28]), and upper and lower 68% C.L. limits for the D-factor of Draco derived in [29].

We consider the COSI angular resolution requirements at 0.511 MeV and 1.809 MeV reported in Table 1 of [25]. Then our approximation for other energies is based on a linear interpolation between 0.511 MeV and 1.809 MeV and a linear extrapolation below 0.511 MeV. We assume a flat angular resolution above 1.809 MeV.

Target	D-factor[1°] MeV cm ⁻²	J-factor[1°] MeV ² cm ⁻⁵
GC	$0.55 - 1.7 \times 10^{23}$	$0.067 - 4.4 \times 10^{27}$
LMC	$1.8 - 2.7 \times 10^{22}$	$1.6 - 5.3 \times 10^{25}$
Draco	$0.52 - 4.5 \times 10^{22}$	$0.83 - 8.0 \times 10^{25}$

Table 1. D- and J-factors at 1° for the targets under investigation. The references used in the computation are [28] (GC) but normalised to a DM density of 0.4 GeV/cm^3 at the Earth location [27], [26] (LMC), and [29] (Draco).

Given the relatively poor angular resolution of COSI, Draco can be considered as a point-like source. In the case of the GC and (to a lesser extent) LMC, it would be desirable to analyze the target as an extended source. For extended sources, dedicated simulations by the COSI Collaboration would be ideal in order to derive the telescope sensitivity. In this work, following the procedure described in [30] (Appendix B), we use the scaling of the sensitivity with the power of 1/4 of the ratio between the extended source area and the beam area. Thus, for extended sources, we compute the D-factor in Eq. 2.3 over the source region Ω_{src} and rescale the point-source sensitivity Φ_{exp} by a factor $(\Omega_{\text{src}}/\Omega_{\text{res}})^{0.25}$, with $\Omega_{\text{res}} = \pi(\text{HWHM}_{\text{ARM}})^2$. For the GC we consider a region of radius of 10° with an improvement of more than one order of magnitude in the bound, with respect to considering a single central beam, while for the LMC we take 5° and the effect is more limited. Results about the sensitivity on the DM parameter space are shown in Fig. 1 (left panel).

Recently, Ref. [24] derived strong bounds on MeV DM using INTEGRAL/SPI observations of a large Galactic region with $|\ell| < 47.5^\circ$ and $|b| < 47.5^\circ$. Our simple extrapolation of the COSI sensitivity for extended sources would be too naive on such a large portion of the sky, and dedicated simulations from the COSI Collaboration are in order to obtain a fair comparison. The bounds from Ref. [24] are thus not included here. On the other hand, assuming the ratio between the INTEGRAL/SPI sensitivity and the COSI one for extended regions to be the same as for the case of point-like sources, we notice that less than 2-years of COSI survey (i.e., less than 6 months of integration time) should suffice to obtain a better sensitivity than the one of INTEGRAL/SPI for 65 Ms (i.e., the integration time of the data used in [24]) at energies around MeV.

We should also stress that a few gamma-ray lines from nuclear transitions fall in the energy range of interest. The list includes nuclear decay chains of the isotopes ^{56}Ni with lines arising at 0.812, 0.847 and 1.238 MeV, ^{60}Fe , with lines at 1.173 and 1.333 MeV, ^{26}Al , with a line at 1.809 MeV, ^{44}Ti with a line at 1.157 MeV, and the 511 keV line from e^+e^- annihilation. Therefore, in a few frequency channels, out of the thousands that can be explored given the energy range and resolution of COSI, the DM signal could be contaminated by these emissions. In these cases, a proper modeling and subtraction of these backgrounds should be pursued, similarly to the approach adopted in [24, 31] with INTEGRAL/SPI

observations. Such analysis is beyond the scope of our work, but we notice that COSI will provide unprecedented sensitivity to characterize these nuclear emission lines [4].

Finally, our bounds apply to any model in which DM radiatively decays into photons. It is however interesting to convert COSI prospects on DM lifetime in forecasts for the specific case of ALPs, with mass m_a and coupling to photons $g_{a\gamma\gamma}$. In Fig. 2 we show COSI prospects for this model assuming the ALPs constitute a fraction F_a of the DM, i.e., being agnostic about the ALPs relic abundance. These limits, for the mass range of interest, apply for coupling as large as $g_{a\gamma\gamma} \simeq 10^{-10} - 10^{-11} \text{GeV}^{-1}$, above which the DM lifetime becomes shorter than the age of the universe. Notice that one could use Fig. 2 to constrain any irreducible axion component that is produced in the early Universe and with a relic abundance today (as done in Ref. [32] considering minimal freeze-in production of axions). Finally, we also highlight that axions in this mass range has been recently shown to be theoretically motivated, as they naturally arise from axiverse theories with dark non-abelian gauge groups [33].

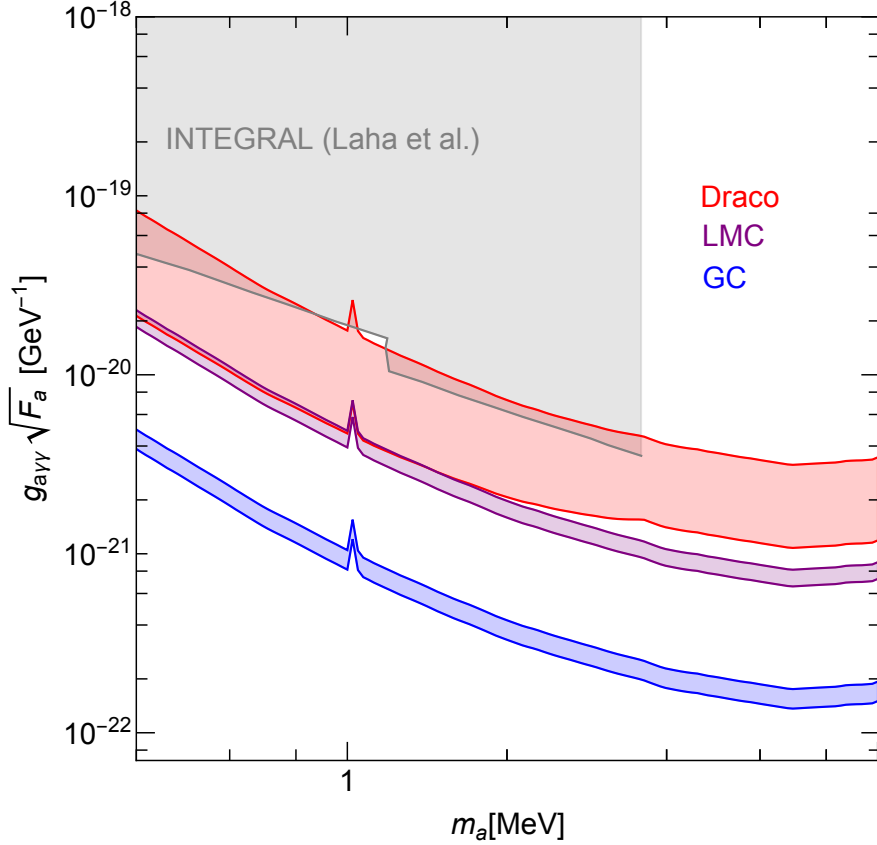


Figure 2. COSI prospects for ALPs constituting a fraction F_a of dark matter and decaying into two photons. As in Fig.1 the three different colors refer to the different targets under consideration (GC, LMC and Draco) and the shaded regions span the two DM density profiles considered in our analysis. The gray shaded region shows existing limits from [23].

2.2 Annihilation

In this section we focus on direct DM annihilation into two photons. The flux, produced at $E_\gamma = m_\chi$, reads:

$$\Phi(E_\gamma) = \frac{\langle \sigma_a v \rangle}{4\pi m_\chi^2} J(\theta), \quad (2.4)$$

where $\langle \sigma_a v \rangle$ is the velocity-averaged annihilation cross-section and the so-called J-factor is:

$$J(\theta) = 2\pi \int_0^\theta d\theta' \sin(\theta') \int dl \rho(l, \theta)^2. \quad (2.5)$$

Using the same arguments as for the decaying DM case, we arrive at the projected sensitivity on the annihilation cross-section:

$$\langle \sigma_a v \rangle = 1.3 \times 10^{-32} \text{ cm}^3/\text{s} \frac{10^{27} \text{ GeV}^2 \text{ cm}^{-5}}{J} \frac{\Phi_{\text{exp}}}{10^{-6} \text{ cm}^2 \text{ s}} \left(\frac{m_\chi}{1 \text{ MeV}} \right)^2 \quad (2.6)$$

where Φ_{exp} is evaluated at $E_\gamma = m_\chi$ and the angular integration for J is given by the COSI angular resolution at E_γ (see some reference values in Table 1). Results are in the right panel of Fig. 1, for the same targets and regions of observations considered in Section 2.1.

Before moving to continuum signals, we notice that Ref. [34] also provided an estimate of the reach of COSI for $\langle \sigma_a v \rangle$. The values obtained by the authors (see their discussion at pag. 14 of Ref. [34]) are significantly more constraining than ours. We checked that this difference is due to a different choice of the J-factor, which was more optimistic in Ref. [34].

3 Continuum signals

We now move to DM scenarios for which a continuum photon signal is expected. This is the case of light DM decaying or annihilating into leptons or mesons, which in turn emit radiation. Another possibility are PBHs, which evaporate producing an (almost) thermal spectrum of photons.

As we mentioned in the introduction, COSI is optimized for the detection of MeV lines. The continuum sensitivity suffers from a larger instrumental background, which limits the detection efficiency. The possibility to constrain the DM scenarios that we have just described are somewhat less promising than for the cases of Section 2, but anyway relevant, and improving on current bounds for some masses, as we describe below.

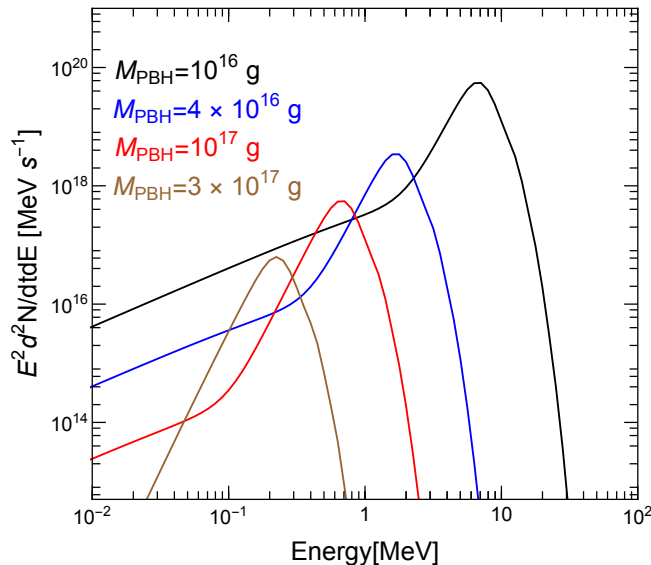


Figure 3. Differential photon emission rate due to Hawking radiation [35] for PBH with different masses. These spectra include both primary and secondary photon emissions (originating from other produced particles, such as electrons) as obtained using the public code BlackHawk [36]. The smaller the PBH mass, the larger the photons peak energy, as it follows from the BH temperature [35] $T_{BH} = \frac{1}{8\pi GM_{BH}} \simeq \text{MeV} \left(\frac{10^{16} \text{g}}{M_{BH}} \right)$.

3.1 Primordial black holes evaporation

The recent detection of gravitational waves from black holes mergers prompted a renewed interest in the possibility that all or a sizeable fraction of the DM in our Universe is constituted by PBHs, that is to say black holes formed in the early universe and not from stellar evolution, see e.g. [17–20] for recent reviews.

In his seminal work Hawking demonstrated that a black hole (BH) is not really black, but actually emits an (almost) thermal spectrum of particles with temperature [35]

$$T_{BH} = \frac{1}{8\pi GM_{BH}} \simeq \text{MeV} \left(\frac{10^{16} \text{g}}{M_{BH}} \right), \quad (3.1)$$

where G is the Newton gravitational constant and M_{BH} the BH mass. In particular, the emission rate of a particle state of spin s and energy ω from a Schwarzschild BH is given by

$$\frac{dN_i}{d\omega dt} = \frac{g_i}{2\pi} \frac{\Gamma_i(\omega, T_{BH})}{e^{\omega/T_{BH}} - (-1)^{2s}}, \quad (3.2)$$

where g_i is the number of internal dof of the i -th particle, ω is its energy, and the function Γ_i denotes the so-called grey factor. The latter is the dimensionless absorption probability for the emitted species. It is in general a complicated function of ω , the PBH mass, the particle's internal dof and its rest mass. In order to compute the associated photon spectrum we make use of the public code BlackHawk [36], including also the photons originating from unstable particles produced during the PBH evaporation (calculated using Hazma [37] to compute the photon spectrum from decays). Denoting the differential photon emission rate by $\frac{d^2 N_\gamma}{dE_\gamma dt}$,

which we show in Fig. 3 for a few PBH masses, the flux of photons with energy E_γ received by the telescope is:

$$\Phi(E_\gamma) = \frac{f_{\text{PBH}} D(\theta)}{4\pi M_{\text{PBH}}} \frac{d^2 N_\gamma}{dE_\gamma dt}, \quad (3.3)$$

where M_{PBH} is the PBH mass, f_{PBH} is the fraction of DM in form of PBHs and $D(\theta)$ is the D-factor integrated over a certain source area of angular size θ as already described above. Notice that in this work we only consider a monochromatic mass distribution for the PBHs. Nevertheless, our analysis can be easily adapted to a different mass function, see e.g. [38].

For a given PBH mass we can then compare the theoretical prediction with the COSI sensitivity and estimate the value of f_{PBH} which can be tested. For the COSI sensitivity in the continuum we use the five points in Figure 4 of Ref. [30] rescaled with a power of 1/4 of the ratio between the source area and an area of 20-degree radius, to take into account the fact that Figure 4 of Ref. [30] refers to the performance for a disk-like source with 20-degree radius (see their Appendix B).

Notice also that those prospects are related to the Fermi Bubbles, i.e., to the central part of the Galaxy. Nevertheless we expect them to be similar in other directions of the sky since the Galactic foreground plays a minor role in the determination of the sensitivity, which is dominated by the instrumental background. The bound on the PBH fraction is therefore computed as

$$f_{\text{PBH}} < \left[\frac{4\pi M_{\text{PBH}}}{D(\theta)} \times \frac{1}{d^2 N_\gamma / dE_\gamma dt} \times \Phi_{\text{exp}}(E_\gamma) \times \left(\frac{\pi \theta^2}{\pi 20^\circ{}^2} \right)^{1/4} \right]_{\text{min}}, \quad (3.4)$$

where $\Phi_{\text{exp}}(E_\gamma)$ is the COSI sensitivity of Ref. [30]. The subscript “min” means that we evaluate the above expression at the five energy bins of Figure 4 in Ref. [30] and then take the minimum value.

We present these prospects for the GC as a shaded red band in Fig. 4 (spanning the two considered density profiles, as done for spectral line signals). For comparison we also show current bounds (solid blue line) from INTEGRAL/SPI observations as taken from Ref. [31]. As evident, COSI will be able to improve present constraints also in this case.

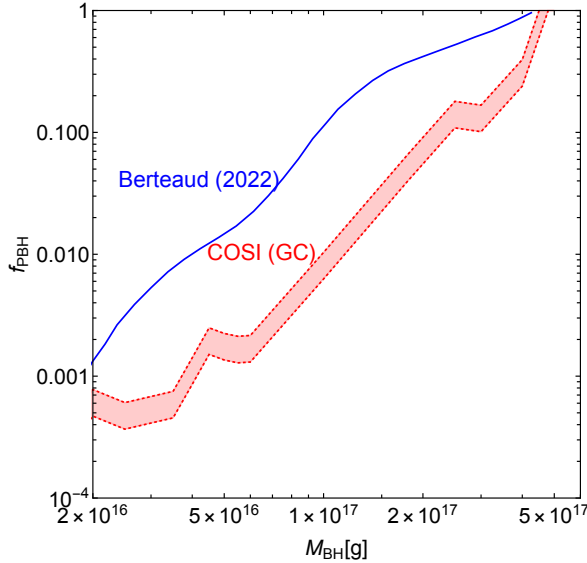


Figure 4. COSI prospects for the detection of PBH Hawking radiation into photons from the GC (shaded red region, which spans the two DM density profiles considered in our analysis). The solid blue line indicates the existing bounds from INTEGRAL/SPI observations, taken from Ref. [31].

3.2 Annihilation and decay of sub-GeV DM into leptons

In Sec. 2 we have considered direct DM decays and annihilations into photons, a scenario particularly promising for COSI, since this telescope is designed to look for gamma-ray lines. Nevertheless, in many motivated models DM annihilates into leptons or mesons, which in turn produce a continuum spectrum of photons. Here, for concreteness, we focus on the simple case of DM annihilating or decaying into electrons and positrons, $\chi\chi \rightarrow e^+e^-$ or $\chi \rightarrow e^+e^-$. For annihilations, the differential photon spectrum [15, 39, 40] is:

$$\frac{dN_{\text{FSR}\gamma}^{e^+e^-}}{dE_\gamma} = \frac{\alpha}{\pi\beta(3-\beta^2)m_\chi} \left[\mathcal{A} \ln \frac{1+R(\nu)}{1-R(\nu)} - 2\mathcal{B}R(\nu) \right], \quad (3.5)$$

where

$$\mathcal{A} = \left[\frac{(1+\beta^2)(3-\beta^2)}{\nu} - 2(3-\beta^2) + 2\nu \right], \quad (3.6)$$

$$\mathcal{B} = \left[\frac{3-\beta^2}{\nu}(1-\nu) + \nu \right], \quad (3.7)$$

and: $\nu = E_\gamma/m_\chi$, $\beta^2 = 1 - 4\mu^2$ with $\mu = m_e/(2m_\chi)$, $R(\nu) = \sqrt{1 - 4\mu^2/(1-\nu)}$ and m_e the electron mass. Given the differential photon spectrum, one can write down the expected flux of photons from a given astrophysical target (say the GC) for self-conjugated DM particles (e.g. Majorana fermions) as:

$$\Phi^{\text{ann}}(E_\gamma) = \frac{J(\theta)}{4\pi m_\chi^2} \times \frac{\langle\sigma v\rangle}{2} \times \frac{dN_{\text{FSR}\gamma}^{e^+e^-}}{dE_\gamma}, \quad (3.8)$$

where $J(\theta)$ is the J-factor for the observed target, m_χ the mass of the annihilating DM and $\langle\sigma v\rangle$ the annihilation cross-section. Notice that if DM is not constituted by self-conjugated particles, an additional factor 1/2 appears.

For decaying DM, the differential photon spectrum is the same as in Eq. (3.5) with the substitution $m_\chi \rightarrow m_\chi/2$ everywhere, and the flux of photons reads

$$\Phi^{\text{dec}}(E_\gamma) = \frac{D(\theta)/\tau}{4\pi m_\chi} \times \frac{dN_{\text{FSR}\gamma}^{e^+e^-}}{dE_\gamma}, \quad (3.9)$$

where $D(\theta)$ is the D-factor and τ the DM lifetime for the decay into electron/positron pairs.

We then proceed to derive the COSI projected sensitivities as for the PBH case. For 2 years of mission time we derive the prospects showed in Fig. 5. COSI forecasts for the GC are shown again as a shaded red band, while present bounds from other experiments such as COMPTEL, EGRET, Fermi and INTEGRAL are shown in solid blue (taken from Figure 1 of Ref. [41]). For comparison we also show the constraints from CMB temperature and polarization anisotropies as black lines [41, 42].

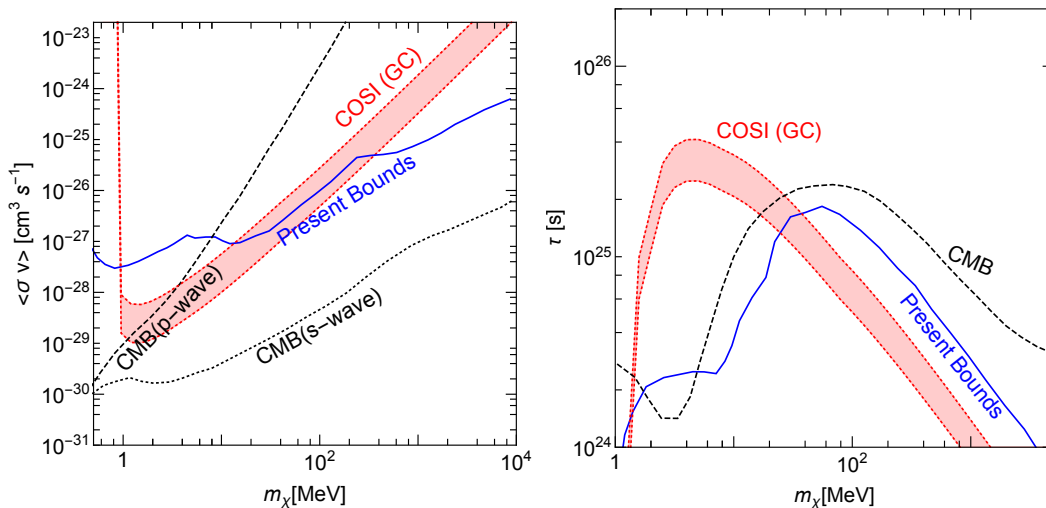


Figure 5. (Left). Projected sensitivity on the DM velocity-averaged annihilation cross-section $\langle\sigma v\rangle$ for the process $\chi\chi \rightarrow e^+e^-$. The COSI prospects for the GC are shown as a shaded band (spanning the two considered density profiles, as in Fig. 1), current gamma-ray bounds are in solid blue (taken from Figure 1 of Ref. [41]) and CMB bounds for s-wave (dotted) and p-wave (dashed) annihilation are in black. (Right) Sensitivity on the lifetime of DM decaying into e^+e^- . The color code is as in the left panel.

4 COSI, dark matter and the Galactic Center 511 keV gamma-ray line

The presence of a 511 keV line from the GC is a long-standing issue, with its first detection dating back to the 1970’s [43, 44]. More recently, the INTEGRAL/SPI experiment observed an emission compatible with the annihilation of $\sim (1.5 \pm 0.1) \cdot 10^{43}$ positrons/s [22] in a region within ~ 1 kpc of the GC. Among conventional sources, there are radioactive ejecta from stars, supernovae and gamma-ray bursts, positrons from pair creation near pulsars or from p-p collisions associated with cosmic rays [45]. Most of the solutions, however, are not completely satisfactory to fully explain the excess. This motivated the investigation of more “exotic” alternatives, some of which trace back to DM to provide the required large number

of positrons. In fact, as discussed in the previous two sections, there are many DM models for which the production of e^+e^- is expected. In these scenarios, low-energy positrons would then annihilate with ambient electrons producing the 511 keV gamma-ray line.

Given its exquisite spectral resolution, COSI will be instrumental in characterizing the 511 keV line at the GC and therefore constraining DM signals. Let us start considering PBH DM as in Sec. 3.1. Given the “democratic” nature of gravity, a PBH generates all possible spectra of particles energetically allowed, and therefore for small enough PBH masses, we also expect a copious production of e^+e^- , which would then contribute to the 511 keV line [46–48]. In order to match the excess, the flux of photons should be $\Phi_{511} \sim 10^{-3}$ ph/cm²/s, which in turn corresponds to a positron luminosity of $L_{e^+} \sim 2 \times 10^{43}$ e⁺/s [22]. However, the injected positrons cannot be too energetic. In fact, a sizeable emission of positrons with energies above ~ 3 MeV could produce an excess of high energy photons due to inflight annihilation [49]. Nevertheless, for the PBH masses that we are considering, we checked that energetic positrons (> 3 MeV) only accounts for a small fraction of the total luminosity and therefore this constraint does not apply.

As for the photon spectrum in Sec. 3.1, we make use of the public code BlackHawk [36] to generate the positron differential rate $dN_{e^+}/d\omega dt$, including both the primary and the secondary contributions. Therefore, the number of positrons from PBH evaporation per unit of time in the energy range of interest can be computed as

$$L_{e^+}^{\text{PBH}} = \frac{f_{\text{PBH}}}{M_{\text{PBH}}} \int dV \rho(r) \int_{m_e}^{\infty} d\omega \frac{dN_{e^+}}{d\omega dt}, \quad (4.1)$$

where for the DM density distribution ρ we have adopted a NFW profile normalized as in Sec. 2. Concerning the volume integral, we assume, as done in previous analyses [46], that all the positrons emitted within 1.5 kpc from the GC contribute to the 511 keV gamma-ray emission, i.e., the integral is limited to distances < 1.5 kpc. Then, Eq. (4.1) can be equated to the experimental measurement $L_{e^+} \sim 2 \times 10^{43}$ e⁺/s [22] to obtain an upper limit on f_{PBH} for a given PBH mass. We notice that the morphology of the signal is not compatible with DM decay (or BH evaporation in this case) [50, 51], but one can still use the measurements to draw limits. A full morphological analysis is likely to provide more stringent bounds.

Following the outlined procedure we obtained the projected limits shown with a dashed red line in Fig. 6. The results are reasonably similar to those of Ref. [46] and the (small) differences are likely due to the fact that Ref. [46] used non-relativistic approximated form for the spectra of fermions produced from PBH evaporation.

We now explore the potential of COSI to constrain a DM contribution to the 511 keV signal, under the assumption that this emission is produced by astrophysical sources, whose nature and properties will be pinpointed by COSI. Therefore, in order to constrain PBHs evaporation, we compare the corresponding signal with the sensitivity of COSI at 511 keV, i.e. the accuracy up to which the astrophysical explanation can be tested. For a region within 5° from the GC, i.e. the size of the detected signal, the 3σ COSI line sensitivity is $\Phi_{511}^{\text{COSI}} \sim 1 \times 10^{-5}$ ph/cm²/s, obtained again from Ref. [25], and re-scaling the point-source sensitivity as described above. This corresponds to a positron luminosity $L_{e^+} \sim 2 \times 10^{41}$ e⁺/s. Using this information, we obtain the projected limits shown with a dotted red curve in Fig. 6, which are roughly 2 orders of magnitude more constraining than current bounds. Clearly, the simple estimate presented here is affected by several sources of uncertainty. First, the propagation of low energy positrons at the GC is not well known. Then, our assessment of the constraining power of COSI might be optimistic (i.e., data perfectly fitted by an

astrophysical explanation), and a precise determination of maximum fraction of the 511 keV emission which can be ascribed to DM signals will be possible only with COSI data at hands. The actual bound will be somewhere in between the dashed and the dotted curves in Fig. 6. Our calculations are in any case an indication that COSI will have the potential to strongly challenge PBH DM in the $10^{16} - 10^{17}$ g mass range.

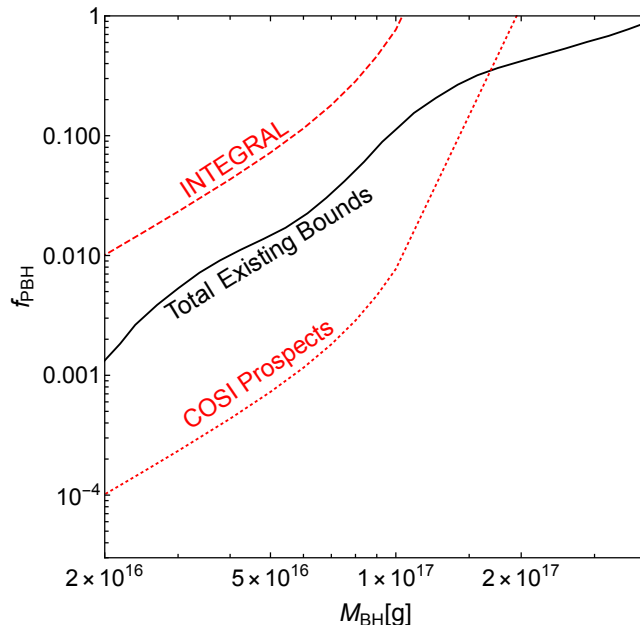


Figure 6. Limit on the fraction of PBH dark matter from the 511 keV emission at the GC. The dashed red curve is obtained following the recipe of Ref. [46], but with a full relativistic treatment for the PBH evaporation spectrum. The solid black line indicates current bounds on f_{PBH} from other observations [31], while the dotted red curve is the prospect for the COSI mission.

Finally, the same procedure adopted for PBH evaporation can also be applied to DM annihilations or decays into electrons and positrons. In these two cases the positron fluxes read

$$\Phi_{e^+}^{\text{ann}} = \frac{1}{2} \frac{4\pi}{m_\chi^2} \langle \sigma v \rangle \int_0^{1.5 \text{kpc}} dr r^2 \rho_{\text{DM}}^2(r), \quad (4.2)$$

$$\Phi_{e^+}^{\text{dec}} = \frac{4\pi}{m_\chi} \frac{1}{\tau} \int_0^{1.5 \text{kpc}} dr r^2 \rho_{\text{DM}}(r). \quad (4.3)$$

For small enough DM masses, below a few MeV, the positrons will not escape the GC and annihilating with ambient electrons will contribute to the 511 keV line signal. Then, one can impose $\Phi_{e^+}^{\text{ann,dec}} < 2 \times 10^{43} \text{ e}^+/\text{s}$ ($2 \times 10^{41} \text{ e}^+/\text{s}$) obtaining the bounds

$$\begin{aligned} \langle \sigma v \rangle &\lesssim 2.3 \times 10^{-30} \text{ cm}^3 \text{ s}^{-1} \left(\frac{m_\chi}{\text{MeV}} \right)^2, \quad \left[2.2 \times 10^{-32} \text{ cm}^3 \text{ s}^{-1} \left(\frac{m_\chi}{\text{MeV}} \right)^2 \right] \\ \tau &> 1.1 \times 10^{26} \text{ s} \left(\frac{\text{MeV}}{m_\chi} \right), \quad \left[1.1 \times 10^{28} \text{ s} \left(\frac{\text{MeV}}{m_\chi} \right) \right]. \end{aligned} \quad (4.4)$$

These limits, derived with a very simple procedure, are overall very similar to those obtained in Ref. [50] where the authors attempted a more sophisticated analysis, modelling

possible astrophysical sources contributing to the 511 keV emission. In Eq. (4.4), in parenthesis we also report the projected limits corresponding to the COSI sensitivity, similarly to what done in Fig. 6 with the dotted line. We do not show the bounds of Eq. (4.4) in Fig. 5, as it is difficult to precisely draw the mass range over which they apply robustly. For masses below a few MeV they can be confidently taken and result to be the strongest ones, competing with CMB constraints even for s-wave annihilations. On the other hand, for larger masses, the description of cooling and diffusion of energetic positrons in the Galaxy becomes crucial, adding a model dependency to the bound.

5 Conclusions

Scheduled to be launched in 2027, COSI will provide us with spectroscopic images of the sky at MeV energy with unprecedented sensitivity. In this work, we discussed how to use these data to constrain different types of DM candidates. We showed that COSI will offer an exquisite possibility to detect DM directly decaying or annihilating into monochromatic gamma-rays, as for the case of ALP DM. Fig. 1 shows that the projected sensitivities for spectral line signatures can lead to a significant improvement of the current bounds.

We also computed the expected sensitivity for continuum signals, such as those produced by PBH evaporation or sub-GeV DM annihilation/decay into leptons. For those scenarios, we found again that the projected limits are more stringent than existing limits.

Finally, we discussed how measurements of the 511 keV line emission at the GC can constrain the injection of positrons from DM. Through this observable, COSI will have the potential to significantly improve current limits, and challenge the hypothesis of PBH DM to extremely small fractional abundances in the $10^{16} - 10^{17}$ g mass range.

The work is intended to provide a first assessment of COSI capabilities related to DM searches. More details about the final design and simulated instrumental responses will be released in the next years by the COSI Collaboration, prior to the stellite launch, and this will allow an improved determination of the projected sensitivities.

Acknowledgements

We want to thank the COSI dark matter topical working group, and in particular we thank Shigeki Matsumoto, Tom Melia, Thomas Siebert, Tadayuki Takahashi for the fruitful discussions and kind support; John Tomsick and Andreas Zoglouer for crucial insights about the COSI instrument and capabilities. AC also thanks William De Rocco for useful discussions about the 511 keV lines and PBH dark matter. AC is supported by the Foreign Postdoctoral Fellowship Program of the Israel Academy of Sciences and Humanities and also acknowledges support from the Israel Science Foundation (Grant 1302/19), the US-Israeli BSF (Grant 2018236), the German-Israeli GIF (Grant I-2524-303.7) and the European Research Council (ERC) under the EU Horizon 2020 Programme (ERC-CoG-2015-Proposal n. 682676 LDMThExp). MN acknowledges NASA support under award number 80GSFC21M0002. MR acknowledges support by the PRIN research grant “From Darklight to Dark Matter: understanding the galaxy/matter connection to measure the Universe” No. 20179P3PKJ funded by MIUR, and by the research grant TAsP (Theoretical Astroparticle Physics) funded by Istituto Nazionale di Fisica Nucleare (INFN). MT acknowledges the research grant “The Dark Universe: A Synergic Multimessenger Approach No. 2017X7X85” funded by MIUR, and the project “Theoretical Astroparticle Physics (TAsP)” funded by Istituto Nazionale di Fisica Nucleare (INFN).

References

- [1] AMEGO Collaboration, R. Caputo et al., *All-sky Medium Energy Gamma-ray Observatory: Exploring the Extreme Multimessenger Universe*, [1907.07558](#).
- [2] e-ASTROGAM Collaboration, M. Tavani et al., *Science with e-ASTROGAM: A space mission for MeV–GeV gamma-ray astrophysics*, *JHEAp* **19** (2018) 1 [[1711.01265](#)].
- [3] A. De Angelis et al., *Gamma-ray astrophysics in the MeV range: The ASTROGAM concept and beyond*, *Exper. Astron.* **51** (2021) 1225 [[2102.02460](#)].
- [4] J. Tomsick, A. Zoglauer, C. Sleator, H. Lazar, J. Beechert, S. Boggs, J. Roberts, T. Siegert, A. Lowell, E. Wulf, E. Grove, B. Philips, T. Brandt, A. Smale, C. Kierans, E. Burns, D. Hartmann, M. Leising, M. Ajello, C. Fryer, M. Amman, H.-K. Chang, P. Jean and P. von Ballmoos, *The Compton Spectrometer and Imager*, in *Bulletin of the American Astronomical Society*, vol. 51, p. 98, Sept., 2019, [1908.04334](#).
- [5] R. Caputo et al., *The All-sky Medium Energy Gamma-ray Observatory eXplorer (AMEGO-X) Mission Concept*, [2208.04990](#).
- [6] A. Takada et al., *First Observation of the MeV Gamma-Ray Universe with Bijective Imaging Spectroscopy Using the Electron-tracking Compton Telescope on Board SMILE-2+*, *Astrophys. J.* **930** (2022) 6 [[2107.00180](#)].
- [7] V. Schoenfelder, H. Aarts and K. Bennett, *Instrument Description and Performance of the Imaging Gamma-Ray Telescope COMPTEL aboard the Compton Gamma-Ray Observatory*, *ApJS* **86** (1993) 657.
- [8] Compton Gamma-Ray Observatory. <https://heasarc.gsfc.nasa.gov/docs/cgro/cgro.html>, 1991.
- [9] G. Vedrenne, J. P. Roques, V. Schönfelder, P. Mandrou, G. G. Lichti, A. von Kienlin, B. Cordier, S. Schanne, J. Knödseder, G. Skinner, P. Jean, F. Sanchez, P. Caraveo, B. Teegarden, P. von Ballmoos, L. Bouchet, P. Paul, J. Matteson, S. Boggs, C. Wunderer, P. Leleux, G. Weidenspointner, P. Durouchoux, R. Diehl, A. Strong, M. Cassé, M. A. Clair and Y. André, *SPI: The spectrometer aboard INTEGRAL*, *A&A* **411** (2003) L63.
- [10] J. Beechert, H. Lazar, S. E. Boggs, T. J. Brandt, Y.-C. Chang, C.-Y. Chu, H. Gulick, C. Kierans, A. Lowell, N. Pellegrini, J. M. Roberts, T. Siegert, C. Sleator, J. A. Tomsick and A. Zoglauer, *Calibrations of the Compton Spectrometer and Imager*, *Nuclear Instruments and Methods in Physics Research A* **1031** (2022) 166510 [[2203.00695](#)].
- [11] C. Boehm, T. A. Ensslin and J. Silk, *Can Annihilating dark matter be lighter than a few GeVs?*, *J. Phys. G* **30** (2004) 279 [[astro-ph/0208458](#)].
- [12] J. F. Beacom, N. F. Bell and G. Bertone, *Gamma-ray constraint on Galactic positron production by MeV dark matter*, *Phys. Rev. Lett.* **94** (2005) 171301 [[astro-ph/0409403](#)].
- [13] D. P. Finkbeiner and N. Weiner, *Exciting Dark Matter and the INTEGRAL/SPI 511 keV signal*, *Phys. Rev. D* **76** (2007) 083519 [[astro-ph/0702587](#)].
- [14] R. Essig, N. Sehgal and L. E. Strigari, *Bounds on Cross-sections and Lifetimes for Dark Matter Annihilation and Decay into Charged Leptons from Gamma-ray Observations of Dwarf Galaxies*, *Phys. Rev. D* **80** (2009) 023506 [[0902.4750](#)].
- [15] R. Essig, E. Kuflik, S. D. McDermott, T. Volansky and K. M. Zurek, *Constraining Light Dark Matter with Diffuse X-Ray and Gamma-Ray Observations*, *JHEP* **11** (2013) 193 [[1309.4091](#)].
- [16] K. K. Boddy and J. Kumar, *Indirect Detection of Dark Matter Using MeV-Range Gamma-Ray Telescopes*, *Phys. Rev. D* **92** (2015) 023533 [[1504.04024](#)].
- [17] B. Carr and F. Kuhnel, *Primordial Black Holes as Dark Matter: Recent Developments*, *Ann. Rev. Nucl. Part. Sci.* **70** (2020) 355 [[2006.02838](#)].

- [18] A. M. Green and B. J. Kavanagh, *Primordial Black Holes as a dark matter candidate*, *J. Phys. G* **48** (2021) 043001 [2007.10722].
- [19] M. Sasaki, T. Suyama, T. Tanaka and S. Yokoyama, *Primordial black holes—perspectives in gravitational wave astronomy*, *Class. Quant. Grav.* **35** (2018) 063001 [1801.05235].
- [20] P. Villanueva-Domingo, O. Mena and S. Palomares-Ruiz, *A brief review on primordial black holes as dark matter*, *Front. Astron. Space Sci.* **8** (2021) 87 [2103.12087].
- [21] A. Ray, R. Laha, J. B. Muñoz and R. Caputo, *Near future MeV telescopes can discover asteroid-mass primordial black hole dark matter*, *Phys. Rev. D* **104** (2021) 023516 [2102.06714].
- [22] J. Knodlseder et al., *The All-sky distribution of 511 keV electron-positron annihilation emission*, *Astron. Astrophys.* **441** (2005) 513 [astro-ph/0506026].
- [23] R. Laha, J. B. Muñoz and T. R. Slatyer, *INTEGRAL constraints on primordial black holes and particle dark matter*, *Phys. Rev. D* **101** (2020) 123514 [2004.00627].
- [24] F. Calore, A. Dekker, P. D. Serpico and T. Siebert, *Constraints on light decaying dark matter candidates from 16 years of INTEGRAL/SPI observations*, 2209.06299.
- [25] COSI Collaboration, J. A. Tomsick, *The Compton Spectrometer and Imager Project for MeV Astronomy*, *PoS ICRC2021* (2021) 652 [2109.10403].
- [26] M. Regis et al., *The EMU view of the Large Magellanic Cloud: troubles for sub-TeV WIMPs*, *JCAP* **11** (2021) 046 [2106.08025].
- [27] E. V. Karukes, M. Benito, F. Iocco, R. Trotta and A. Geringer-Sameth, *Bayesian reconstruction of the Milky Way dark matter distribution*, *JCAP* **09** (2019) 046 [1901.02463].
- [28] M. Cirelli, G. Corcella, A. Hektor, G. Hutsi, M. Kadastik, P. Panci, M. Raidal, F. Sala and A. Strumia, *PPPC 4 DM ID: A Poor Particle Physicist Cookbook for Dark Matter Indirect Detection*, *JCAP* **03** (2011) 051 [1012.4515]. [Erratum: JCAP 10, E01 (2012)].
- [29] V. Bonnivard et al., *Dark matter annihilation and decay in dwarf spheroidal galaxies: The classical and ultrafaint dSphs*, *Mon. Not. Roy. Astron. Soc.* **453** (2015) 849 [1504.02048].
- [30] M. Negro, H. Fleischhack, A. Zoglauer, S. Digel and M. Ajello, *Unveiling the Origin of the Fermi Bubbles with MeV Photon Telescopes*, *Astrophys. J.* **927** (2022) 225 [2111.10362].
- [31] J. Berteaud, F. Calore, J. Iguaz, P. D. Serpico and T. Siebert, *Strong constraints on primordial black hole dark matter from 16 years of INTEGRAL/SPI observations*, *Phys. Rev. D* **106** (2022) 023030 [2202.07483].
- [32] K. Langhoff, N. J. Outmezguine and N. L. Rodd, *The Irreducible Axion Background*, 2209.06216.
- [33] J. W. Foster, S. Kumar, B. R. Safdi and Y. Soreq, *Dark Grand Unification in the Axiverse: Decaying Axion Dark Matter and Spontaneous Baryogenesis*, 2208.10504.
- [34] T. Aramaki et al., *Snowmass2021 Cosmic Frontier: The landscape of cosmic-ray and high-energy photon probes of particle dark matter*, 2203.06894.
- [35] S. W. Hawking, *Black hole explosions*, *Nature* **248** (1974) 30.
- [36] A. Arbey and J. Auffinger, *BlackHawk: A public code for calculating the Hawking evaporation spectra of any black hole distribution*, *Eur. Phys. J. C* **79** (2019) 693 [1905.04268].
- [37] A. Coogan, L. Morrison and S. Profumo, *Direct Detection of Hawking Radiation from Asteroid-Mass Primordial Black Holes*, *Phys. Rev. Lett.* **126** (2021) 171101 [2010.04797].
- [38] B. Carr, M. Raidal, T. Tenkanen, V. Vaskonen and H. Veermäe, *Primordial black hole constraints for extended mass functions*, *Phys. Rev. D* **96** (2017) 023514 [1705.05567].

- [39] M. Cirelli, N. Fornengo, B. J. Kavanagh and E. Pinetti, *Integral X-ray constraints on sub-GeV Dark Matter*, *Phys. Rev. D* **103** (2021) 063022 [[2007.11493](#)].
- [40] Y. M. Bystritskiy, E. A. Kuraev, G. V. Fedotovitch and F. V. Ignatov, *The Cross sections of the muons and charged pions pairs production at electron-positron annihilation near the threshold*, *Phys. Rev. D* **72** (2005) 114019 [[hep-ph/0505236](#)].
- [41] A. Coogan, A. Moiseev, L. Morrison and S. Profumo, *Hunting for Dark Matter and New Physics with (a) GECCO*, [2101.10370](#).
- [42] T. R. Slatyer and C.-L. Wu, *General Constraints on Dark Matter Decay from the Cosmic Microwave Background*, *Phys. Rev. D* **95** (2017) 023010 [[1610.06933](#)].
- [43] I. Johnson, W. N., J. Harnden, F. R. and R. C. Haymes, *The Spectrum of Low-Energy Gamma Radiation from the Galactic-Center Region.*, *ApJL* **172** (1972) L1.
- [44] M. Leventhal, C. J. MacCallum and P. D. Stang, *Detection of 511 keV positron annihilation radiation from the galactic center direction.*, *ApJL* **225** (1978) L11.
- [45] N. Prantzos et al., *The 511 keV emission from positron annihilation in the Galaxy*, *Rev. Mod. Phys.* **83** (2011) 1001 [[1009.4620](#)].
- [46] R. Laha, *Primordial Black Holes as a Dark Matter Candidate Are Severely Constrained by the Galactic Center 511 keV γ -Ray Line*, *Phys. Rev. Lett.* **123** (2019) 251101 [[1906.09994](#)].
- [47] W. DeRocco and P. W. Graham, *Constraining Primordial Black Hole Abundance with the Galactic 511 keV Line*, *Phys. Rev. Lett.* **123** (2019) 251102 [[1906.07740](#)].
- [48] G. M. Fuller, A. Kusenko and V. Takhistov, *Primordial Black Holes and r-Process Nucleosynthesis*, *Phys. Rev. Lett.* **119** (2017) 061101 [[1704.01129](#)].
- [49] J. F. Beacom and H. Yuksel, *Stringent constraint on galactic positron production*, *Phys. Rev. Lett.* **97** (2006) 071102 [[astro-ph/0512411](#)].
- [50] A. C. Vincent, P. Martin and J. M. Cline, *Interacting dark matter contribution to the Galactic 511 keV gamma ray emission: constraining the morphology with INTEGRAL/SPI observations*, *JCAP* **04** (2012) 022 [[1201.0997](#)].
- [51] Y. Ascasibar, P. Jean, C. Boehm and J. Knoedseder, *Constraints on dark matter and the shape of the Milky Way dark halo from the 511-keV line*, *Mon. Not. Roy. Astron. Soc.* **368** (2006) 1695 [[astro-ph/0507142](#)].